Resilient Structures and Sustainable Construction
Edited by Pellicer, E., Adam, J. M., Yepes, V., Singh, A., and Yazdani, S.

ISBN: 978-0-9960437-4-8

SEISMIC BEHAVIOR OF POST-TENSIONED ROCKING COLUMNS WITH RE-PLACEABLE ENERGY DISSIPATERS

H. H. HUNG[1], C. W. HUANG[2], and C. R. JIANG[1]

[1]*National Center for Research on Earthquake Engineering, Taipei, Taiwan*
[2]*Dept of Civil Engineering, Chung Yuan Christian University, Taoyuan City, Taiwan*

To mitigate the column damage during seismic events and to reduce the recovery time after a major earthquake, a post-tensioned bridge column with a rocking interface above the foundation and externally-installed energy dissipation devices was proposed. The energy dissipation devices were specially designed to serve as fuse elements that can be easily replaced after yielding. In addition, a mechanical joint that can rotate freely in all directions was incorporated at one end of the dissipater to ensure bending was not transmitted into this device. To verify the seismic performance of the proposed system, two proposed specimens with different prestressing forces and design details in the rocking base were constructed and tested. From the experiments, it was found that the proposed post-tensioned specimens suffered minor damage after cyclic loadings. All of the damage was concentrated on the inelastic deformation that occurred at the external energy dissipaters. The ease of replacement for the external energy dissipaters was also confirmed.

Keywords: Rocking mechanism, Prestressing forces, Cyclic loading, Residual drift.

1 INTRODUCTION

In the wake of the rapid economic growth and advancements in design technology seen in recent years, the seismic design philosophy of bridges has gradually evolved from the assurance of life-safety by preventing collapse during a major earthquake to the maintenance of acceptable serviceability after a major seismic event. Previously, the mainstream seismic design methodology for bridges was ductility design by allowing bridges to deform inelastically to dissipate energy and maintain appropriate strength during severe earthquake attack. Thus, after a severe earthquake, bridge columns have most likely suffered severe damage and traffic interruption is unavoidable while bridges are retrofitted or rebuilt. As a consequence, in order to ensure post-earthquake functionality and to reduce the retrofit cost, designs that reduce the residual displacements and enhance the residual performance of the bridge after an earthquake have become crucial for the new generation of seismic design for bridges. According to a previous study, the rocking mechanism of a properly designed shallow foundation can effectively reduce the seismic demand, and thereby prevent the severe damage of a column at the plastic hinge area (Hung *et al.* 2014). However, a pure rocking mechanism lacks reliable energy dissipation mechanisms and may induce large displacements. In order to enjoy the advantages of a rocking mechanism while preserving proper energy dissipation capacity and having a controllable rocking motion, the use of unbonded post-tensioned/ pre-tensioned columns with

rocking interfaces and supplemental energy dissipation devices has become a promising solution (Roha and Reinhorn 2010, Palermo and Mashal 2012). Based on a similar concept, this study proposed a post-tensioned rocking column with external energy dissipaters. The column was prestressed by unbonded post-tensioned tendons to ensure self-centering behavior and the supplemental energy dissipaters were easily replaced to reduce post-earthquake recovery time for bridges. The energy dissipaters were obtained from steel bars with a reduced diameter over a specific length and the dissipation was provided by the hysteresis of the material due to axial elongation. To ensure that the dissipater was only subjected to axial forces and bending was not transmitted into the dissipaters, a mechanical joint that can rotate freely in all directions is also incorporated at one end of the dissipaters. To investigate the seismic performance of the proposed system, two specimens with different prestressing forces and rocking base details were constructed and tested at the National Center for Research on Earthquake Engineering (NCREE) in Taiwan. For comparison, a conventional cast-in-place monolithic column specimen without connections was also constructed and tested.

2 SPECIMEN DESIGN

Two post-tensioned bridge column specimens denoted as RB-P1 and RB-P2 were prefabricated at NCREE. These two specimens differed in post-tensioning forces and design details in the rocking base as shown in Figure 1 (a) and (b). The design post-tensioning forces for RB-P1 and RB-P2 were $0.04f_c'A_g$ and $0.07f_c'A_g$, respectively. Herein, A_g is the gross cross-sectional area of the column, and f_c' is the concrete compressive strength of the column. In addition, specimen RB-P2 had a 60 cm square neoprene pad with a thickness of 3 cm placed at the interface between the foundation and the bottom segment to release the high compression forces that may arise at the rocking toes. In order to realize the seismic resistance of the current proposed system as compared to the one with the conventional design details, a conventional cast-in-place monolithic column specimen (BM01) was also constructed and tested. As can be observed in Figure 1, all specimens are 3.6 m in effective height with a cross section of 60 cm × 60 cm. The equivalent monolithic specimen BM01 was reinforced with 16-D19 SD420 rebars and transversely reinforced with D13@10 cm perimeter hoops and internal stirrups. Both RB-P1 and RB-P2 specimens were reinforced with 12-D19 SD420 rebars and one tendon. However, only tendons were passed through the interface between the column and foundation. The tendons for specimens RB-P1 and RB-P2 comprised of 8 and 12 seven-wire strands, respectively. The strands were made of steel equivalent to ASTM A416 Grade 270 and each strand had a nominal diameter of 15.2 mm. Specimens RB-P1 and RB-P2 were precast in advance and were separated into 3 segments, including two column segments and a precast foundation. Each column segment was precast with one 15 cm PVC duct within the center to allow tendons to pass through. In addition, both the bottom column segment and the foundation were precast with several threaded rods in the proper locations for the subsequent connection with the external replaceable energy dissipaters, as shown in Figure 2(a) and (b). To provide protection for the highly strained cover concrete during rocking, the edge of the rocking base of the precast column element was chamfered to a chamfer distance of 5 cm (Figure 2c). In addition, 5 mm steel plates were cast into the top surface of the foundation and the bottom surface of the bottom column segment to give the rocking surface sufficient strength for repeated rocking motions.

Figure 3 schematically shows the design details of the energy dissipaters. For the ease of replacement, the energy dissipater was separated into 4 parts and connected by mechanical joints or bolts. The major part (Part II) was fabricated from 32 mm JIS S450 steel bar with a fused diameter of 20 mm over a length of 220 mm. A 40 mm (outside diameter) steel tube, with a wall

thickness of 2 mm, was located over the machined area and epoxy was injected into the space between the tube and bar. The top end of Part II was bolted to a steel bracket (Part I) that was mounted on the side of the precast column. Part III was connected to Part II and Part IV by couplers. Part IV was bolted to the top of the foundation through the precast threaded rods. A specially designed mechanical joint that can rotate freely in all directions was located between Part III and Part IV. Prior to specimen testing, the energy dissipaters were tested to characterize their energy dissipation capacity. The cyclic loading test results are given in Figure 4.

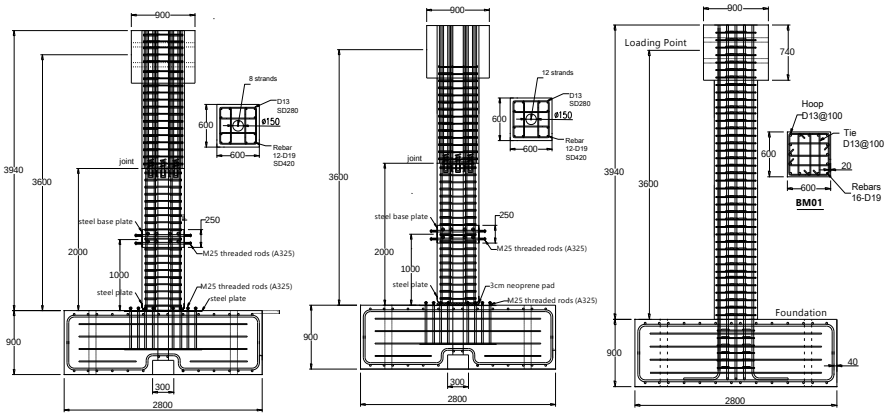

(a) (b) (c)

Figure 1. Design details of specimens (a) RB-P1; (b) RB-P2; (c) BM01 (unit: mm).

(a) (b) (c)

Figure 2. Photos of the precast segment of the proposed specimens (a) column segment; (b) foundation segment; (c) base of the column segment.

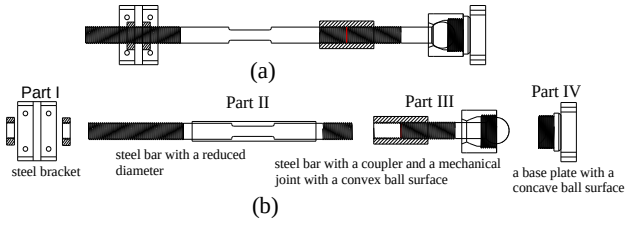

Figure 3. Design details of the energy dissipaters: (a) fully assembled view (b) exploded view.

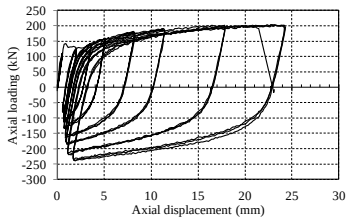

Figure 4. Cyclic testing results of the energy dissipaters.

Specimens RB-P1 and RB-P2 were constructed by stacking precast segments on top of each other with reinforcing bar passing through the interface between two column segments and then

connecting the assembly structure with tendons. After the tendons were prestressed to a predetermined value, and the axial forces representing the dead load of the superstructures were applied, the energy dissipaters were externally installed to the precast specimens. The assembly process of the energy dissipaters is given in Figure 5. Firstly, the base plates with a concave ball surface (Part IV) were bolted to the top of the foundation, and the steel brackets (Part I) were bolted to column through the precast threaded rods. Secondly, the steel bars with a coupler and a mechanical joint with a convex ball surface (Part III) were connected to Part IV by mechanical couplers. Then, the top ends of the major part of the dissipaters (Part II) were passed through the steel brackets from the bottom side. After the position of Part II was adjusted to the correct position, the bottom ends of the Part II were connected to Part III by couplers and the top ends were connected to brackets through bolting. Figure 5(e) is the complete photo.

Step 1 Step 2 step 3 step 4 step 5

Figure 5. Assembly process of the energy dissipaters.

3 EXPERIMENTAL PROGRAM

Displacement-controlled cyclic loading tests were conducted on these specimens. During the test, a constant axial load of 1260 kN, which was around $0.1f_c'A_g$, was applied to the test column through a tap beam to simulate the tributary dead load of the deck. In addition, one horizontal actuator was used to apply the lateral force to the column's top to simulate the seismic loading. The location of the application force was 3.6 m up from the top of the footing. In order to verify the replaceability of the external energy dissipaters, two cyclic tests were conducted on each of the post-tensioned specimens. The first cyclic test stopped after the third cycle of 3.5% drift. At this instant, the outermost energy dissipaters were expected to rupture. Thus, all the energy dissipaters were replaced and the second cyclic test was performed afterwards. It should be noted that only the major part of the energy dissipater (Part II) needs to be replaced. The other parts can remain in use. The first test and second test of specimen RB-P1 are denoted as RB-P1-1 and RB-P1-2, respectively. Similarly, tests for specimen RB-P2 are denoted as RB-P2-1 and RB-P2-2.

4 TEST RESULTS

Figure 6 shows the load-displacement curve for each specimen. For tests RB-P1-1 and RB-P2-1, the outermost external energy dissipaters started to fracture at a drift of 3.5% and a sudden loss in strength can be observed in the load-displacement curves. The tests stopped after the second cycle of the 3.5% drift. At this point, all the energy dissipaters were replaced with new ones and the second tests were conducted afterwards. The test results for the second tests are also given in Figure 6. As can be seen, the hysteresis behavior for the second tests was almost consistent with that of the first tests as the drift was less than or equal to 3.5%. This observation confirmed the quick recovery of the columns through the replacement of damaged external energy dissipaters after a strong earthquake. For the second test, as the drift ratio continued to increase, the strength of the column gradually decreased as the energy dissipaters fractured successively. After the

second cycles of 6% drift, all of the energy dissipaters had ruptured. However, the entire vertical load bearing capacity of the system was still maintained at this time due to the strength contribution from the prestressing forces. By comparing the hysteretic curves of the proposed specimens with that of the specimen BM01, specimen BM01 exhibited more energy dissipation as its hysteresis curve seems fuller. However, the residual displacements for the proposed specimens were much smaller than that of specimen BM01. Both specimens RB-P1 and RB-P2 exhibited flag-shaped hysteretic behavior. The nonlinear behavior was a result of the opening at the rocking base and the material nonlinearity caused by the action of the energy dissipaters.

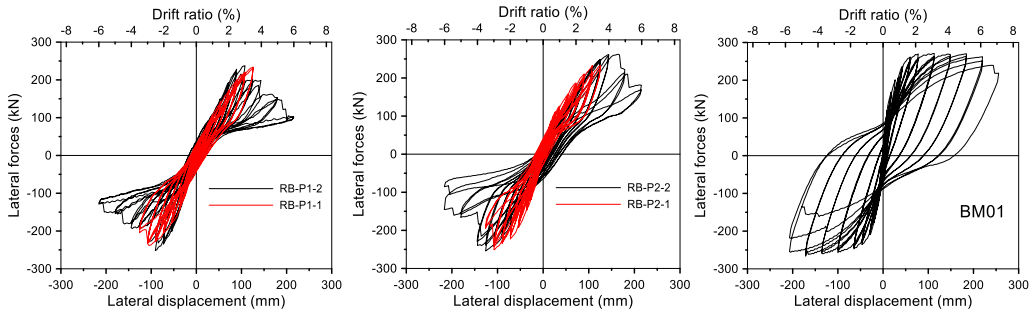

Figure 6. Load-displacement hysteretic curves for specimen (a) RB-P1 (b) RB-P2 (c) BM01.

To quantitatively evaluate the difference between the responses of these three specimens, the equivalent stiffness K_{eff} and equivalent viscous damping ratios ζ_{eq} corresponding to the lateral force-displacement curves were computed using Eq. (1) and displayed in Figure 7(a) and (b).

$$K_{eff} = \frac{F_p - F_n}{\Delta_p - \Delta_n}, \qquad \zeta_{eq} = \frac{E_D}{2\pi K_{eff} {\Delta_0}^2} \tag{1}$$

Where Δ_p and Δ_n = maximum positive and negative displacement of the loop, respectively; F_p and F_n = lateral forces at Δ_p and Δ_n, respectively; Δ_0 = average displacement amplitude of each cycle; and E_D = energy dissipation per cycle or area of the hysteresis loop.

As shown in Figure 7(a), an important difference of the proposed column is the smaller initial stiffness for both specimens RB-P1 and RB-P2 as compared to that of the benchmark specimen as the drift ratio is less than 3. However, the equivalent stiffness of the standard column becomes close to that of the proposed column over 3.5% drift because the stiffness of the standard column deteriorates due to failure of the concrete. Figure 7(b) shows that the computed damping ratios of the benchmark specimen are larger than those of both proposed specimen as the drift larger than 1%, and the damping ratios of the specimen RB-P2 are larger than those of the specimen RB-P1 because the rubber pad located between the column base and foundation can help to dissipate energy. This implies that the energy dissipation capacity for both proposed specimens is not as good as that of the benchmark specimen. However, the residual drifts observed in Figure 7(c) show a different trend. It indicates that the residual drifts of both proposed specimens are much less than those of the BM01, especially at the higher drifts. In addition, from the failure photos (Figure 8) taken after 6% drift, one can find that the damage for RB-P1 was limited to a minor crack of the cover concrete. For RB-P2, where a neoprene pad was inserted between the rocking base and the foundation, only hairline cracks can be observed. On the other hand, for BM01, both vertical and transverse reinforcements were exposed, many longitudinal bars were buckled,

and the bulging of the rectilinear hoops was severe. It is obvious that the limited damage observed from the proposed specimens is advantageous for a bridge design to reduce the recovering time after an extreme earthquake, while the damage observed in the benchmark specimen is not easily repaired immediately after an earthquake.

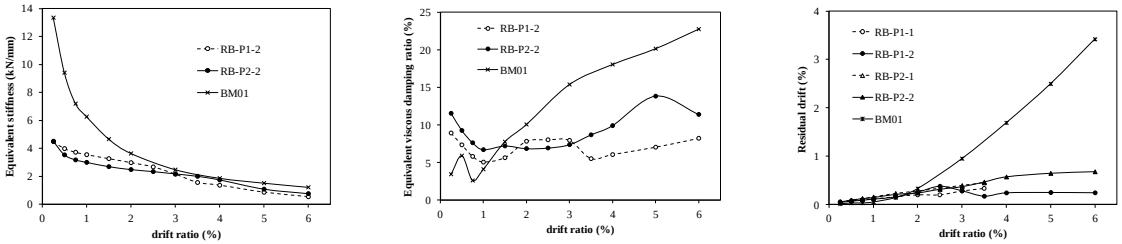

(a) (b) (c)

Figure 7. Comparisons: (a) equivalent stiffness; (b) equivalent viscous damping ratio; (c) residual drift.

(a) (b) (c)

Figure 8. Photographs of the specimens after cyclic loading tests: (a) RB-P1; (b) RB-P2; (c) BM01.

5 CONCLUSIONS

This paper investigates the seismic behavior of two post-tensioned rocking column specimens with replaceable energy dissipaters by performing cyclic loading tests. From the experimental results, the benefits of the rocking column base in limiting damage to the column and external energy dissipater in absorbing earthquake energy were recognized. The advantage of the external energy dissipaters being replaceable after a strong earthquake was also confirmed.

Acknowledgments

The research reported herein is sponsored by the National Center for Research on Earthquake Engineering (NCREE) in Taiwan. The facilities and technical support from NCREE are also gratefully acknowledged.

References

Hung, H. H., Liu, K. Y., and Chang, K.C., Rocking Behavior of Bridge Piers with Spread Footings Under Cyclic Loading and Earthquake Excitation, *Earthquakes and Structures*, 7(6), 1001-1024, 2014.

Roha, H., and Reinhorn, A. M., Modeling and Seismic Response of Structures with Concrete Rocking Columns and Viscous Dampers, *Engineering Structures*, 32(8), 2096–2107, 2010.

Palermo, A., and Mashal, M., Accelerated Bridge Construction (ABC) and Seismic Damage Resistant Technology: A New Zealand Challenge, *Bulletin of the New Zealand Society for Earthquake Engineering*, 45(3), 123-134, 2012.